Near-field optical imaging of abasic sites on a single DNA molecule

JongMin Kim[a], Hiroshi Muramatsu[b], HeaYeon Lee[a,*], Tomoji Kawai[a,*]

[a] *ISIR-Sanken, Osaka University, 8-1 Mohogaoka, Ibaraki, Osaka 567-0047, Japan*
[b] *School of Bionics, Tokyo University of Technology, Katakura, Hachioji, Tokyo 192-0982 Japan*

Received 26 September 2003; revised 3 November 2003; accepted 3 November 2003

First published online 14 November 2003

Edited by Horst Feldmann

Abstract Scanning near-field optical microscopy (SNOM) imaging was performed to allow for the direct visualization of damaged sites on individual DNA molecules to a scale of a few tens of nanometers. Fluorescence in situ hybridization on extended DNA molecules was modified to detect a single abasic site. Abasic sites were specifically labelled with a biotinlylated aldehyde-reactive probe and fluorochrome-conjugated streptavidin. By optimizing the performance of the SNOM technique, we could obtain high contrast near-field optical images that enabled high-resolution near-field fluorescence imaging using optical fiber probes with small aperture sizes. High-resolution near-field fluorescence imaging demonstrated that two abasic sites within a distance of 120 nm are clearly obtainable, something which is not possible using conventional fluorescence in situ hybridization combined with far-field fluorescence microscopy.

Key words: Scanning near-field optical microscopy; DNA damage; DNA imaging; Avidin–biotin interaction

1. Introduction

Scanning near-field optical microscopy (SNOM), a form of scanning probe microscopy, uses a near-field light source as an imaging mechanism and can provide sub-wavelength resolution under various conditions; see for review, for example, [1]. Conventional SNOM can simultaneously produce shear-force and optical images. This dual capacity means that the SNOM image can, in principle, provide more information about a sample than the force image alone. We are developing an imaging system called scanning near-field optical/atomic-force microscopy (SNOM/AFM) in which a bent optical fiber probe is used as a cantilever [2]. Both feedback methods have their different merits. The SNOM/AFM, however, has certain advantages with soft samples and can provide better resolution of a topographic image than that of the normal shear-force-controlled SNOM because of its round tip shape [2], although high-resolution optical imaging for small biosamples remains unsatisfactory.

*Corresponding authors. Fax: (81)-6-6875 2440.
E-mail addresses: hylee@sanken.osaka-u.ac.jp (H. Lee), kawai@sanken.osaka-u.ac.jp (T. Kawai).

Abbreviations: SNOM, scanning near-field optical microscopy; AP, apurinic/apyrimidinic; A532, alexa 532; FWHM, full width half maximum

DNA lesions are an important source of biological mutations. One of the most prevalent sites of DNA damage is at an abasic site, also called an apurinic/apyrimidinic (AP) site, where a DNA base residue is subsequently removed [3,4]. These abnormal sites can be formed from spontaneous depurination, deamination, ionizing radiation or from repair mechanisms in plants and animals [5–7]. The abasic sites can potentially cause carcinogenesis, in addition to cellular death [8]. Since the DNA damage sustained from one DNA molecule to another is different, a sensitive and reliable method to detect AP sites on individual DNA molecules is fundamentally essential in the field of genetic studies.

The visualization of specific DNA molecules can provide for a more detailed study of various DNA mechanisms including DNA transcription, repair and recombination [5–7]. For example, Michalet et al. visualized specific sequences on extended DNA molecules [9]. Lin et al. developed whole-genome optical mapping of *Deinococcus radiodurans* [10]. Furthermore, the direct visualization of abasic sites has been performed by Hirose et al. using far-field fluorescence techniques [11]. One drawback of the far-field technique is its limitation in optical resolution. For example, the precise detection of short sequences or sequence-specific function composed of only a few codons is difficult since far-field optical resolution at room temperature cannot be improved to values below 300 nm [1], which corresponds to a DNA length of approximately 1 kb. Recently, Winkler et al. combined chromosome fluorescence in situ hybridization with SNOM [12], however, a similar methodology applied to DNA related investigations using SNOM has not been reported. Here, we report for the first time high-resolution near-field fluorescence imaging of abasic sites on DNA molecules.

2. Materials and methods

2.1. Abasic DNA sample

A schematic flow diagram representing the preparation of the abasic DNA sample is illustrated in Fig. 1. Target DNA molecules containing abasic sites were prepared by incubating λ-DNA (Wako pure Chemicals, Inc., Japan) in sodium citrate buffer (100 mM NaCl, 10 mM sodium citrate, pH 5.0) at 70°C for 90 min. Following this, 10 μl of 10 mM aldehyde-reactive probe-conjugated biotin (ARP-biotin, 445 Da, Dojindo, Japan) solution was added to 10 μl of the abasic DNA solution (50–100 ng/μl) and the mixture was incubated at 37°C for 1 h. The solution was then purified by passage through a gel filtration column (chroma spin TE-1000, BD Biosciences Clontech, Inc.). Ten μl of a 1/5000 diluted streptavidin solution (s11224, ~52 kDa, Molecular Probe Inc.) labeled with alexa 532 dye (A532, 4 mol of dye per protein in a manufacturer's solution test, adsorption max: 532 nm, emission max: 554 nm, Molecular Probe Inc.) was added to 10 μl of the biotinylated DNA solution and incubated at 37°C for 1 h. The DNA–streptavidin complex was purified by passage through a gel

0014-5793/03/$22.00
doi:10.1016/S0014-5793(03)01298-5

filtration column. The final DNA–streptavidin solution was mixed with a DNA intercalator dye molecule (YOYO-1, adsorption max: 491 nm, emission max: 509 nm, Molecular Probe Inc.) and spin-coated to stretch the DNA molecules [13] on a γ-APTES (3-(amino-propyl)triethoxysilane)-coated mica substrate [14,15]. The mixing ratio of YOYO-1:bp was 1:5, and a spin speed of 5500 rpm was used for stretching the DNA molecules. The depurination treatment does not affect DNA fragmentation under these conditions but randomly generates a few abasic sites on the DNA molecules as reported by Hirose et al. [11].

2.2. SNOM instruments

The SNOM/AFM instrument is based on a conventional AFM unit (SPI 3800, Seiko Instruments Inc), which is capable of a dynamic force mode (DFM) function [14] and uses a bent-type optical fiber probe to enable AFM feedback by a beam deflection method. Light consisting of 488 nm from a multi-line Ar ion laser and 532 nm from a Nd YAG laser with an output power of ~40 mW was coupled to one end of the optical probe and illuminated from the tip of the probe to the sample surface. After transmission through the aperture of the optical fiber probe, the sample and an optical filter set, the remaining light was collected by an avalanche photo diode (EG&G, SPCM-AQR-16). Fluorescence signals collected ranged from 510–650 nm and 540–650 nm for YOYO-1 and A532 molecules, respectively. In an effort to achieve high resolution imaging we modified the system [15] with respect to the scanning unit and the optical fiber probe. Two technical modifications were applied for the scanning unit. To enhance the optical efficiency of the imaging system, self-made optical filter sets were used for imaging YOYO-1 and the A532 dye. Insofar as disturbing the movement of the sample when changing the optical filter sets was concerned, the sample stage was magnetized, and the sample was fixed on a steel ring to attach it firmly on the magnetic sample stage. Thin step-etched optical fiber probes were used for the imaging [16]. The difference between normal optical fiber and the step-etched probes has to do with the spring constant. Due to the low spring constant, the step-etched probes were originally used for contact mode operation but not examined under normal DFM operation. To obtain maximum optical performance, the tip (corn) angle of the optical fiber probe was maximized to enhance the optical transmission efficiency using a multi-mode optical fiber and a special etching method. Using the same tip angle, Hosaka et al. demonstrated 15 nm optical resolution for single molecular fluorescence imaging [17]. The detailed manufacturing process of the probe will be discussed elsewhere.

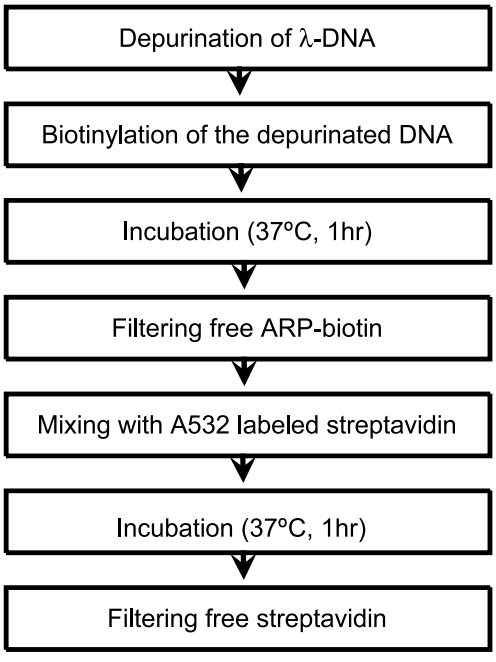

Fig. 1. Procedure used for visualizing abasic sites on λ-DNA molecules.

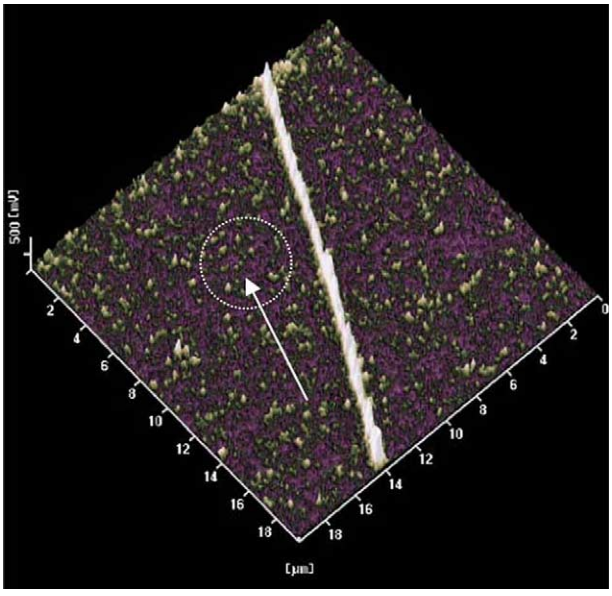

Fig. 2. Highly contrasted near-field fluorescence image showing free YOYO-1 (λ_{exc} = 488 nm) on the background. The image area is 20×20 μm^2 with a 512×256 data format. The optical resolution of free YOYO-1 molecules and DNA width directions is varied. For the free YOYO-1 optical resolution, see the arrow head in the dashed circle. Scanning was performed at a scanning speed of 0.2 Hz and fluorescence gate time of 10 ms. A fluorescence signal of 1 V corresponds to 256 C/10 ms.

3. Results and discussion

Previously we demonstrated that simultaneous high-resolution topography and fluorescence imaging is possible for YOYO-1 intercalated λ-DNA molecules using SNOM/AFM [15]. The location of the intercalated YOYO-1 molecules was clearly observed when the aperture size of the optical probe used was larger than 50 nm. When aperture sizes below this value were used, the signal-to-noise ratio critically decreased and successful near-field imaging of the intercalated YOYO-1 was difficult. This is also one of the general problems in normal SNOM imaging [1]. By optimizing the performance of SNOM/AFM as mentioned above, it is possible to obtain high-contrast near-field fluorescence images.

Fig. 2 shows an example of high-contrast near-field fluorescence imaging for the YOYO-1 intercalated λ-DNA molecule (1 V = 256 C/10 ms). The intercalation of YOYO-1 is controlled by a mixing ratio of 5 bp:1 dye, as recommended by the manufacturer. The length of the λ-DNA molecule was evaluated to about 21 μm by a direct fluorescence length analysis of the DNA length direction. As reported by Bennink et al. [18], the length of the DNA molecules produced can vary depending on the applied stretching force or the YOYO-1 intercalation conditions. When the applied stretching force is strong, the length of a single λ-DNA molecule produced can reach up to 24 μm as shown by Nakao et al. [19]. In the case of spin-stretching, a standard deviation of 16.9 ± 4.3 μm for λ-DNA molecules has been reported [13] at a spin speed of 5500 rpm. Furthermore, it has been confirmed that a similar fluorescence intensity is obtained from the whole DNA length, which is evidence confirming the presence of a single DNA molecule [20]. The fluorescence signal intensity of the single DNA molecule was more than five-fold stronger than that of a previous report [15] at the same optical

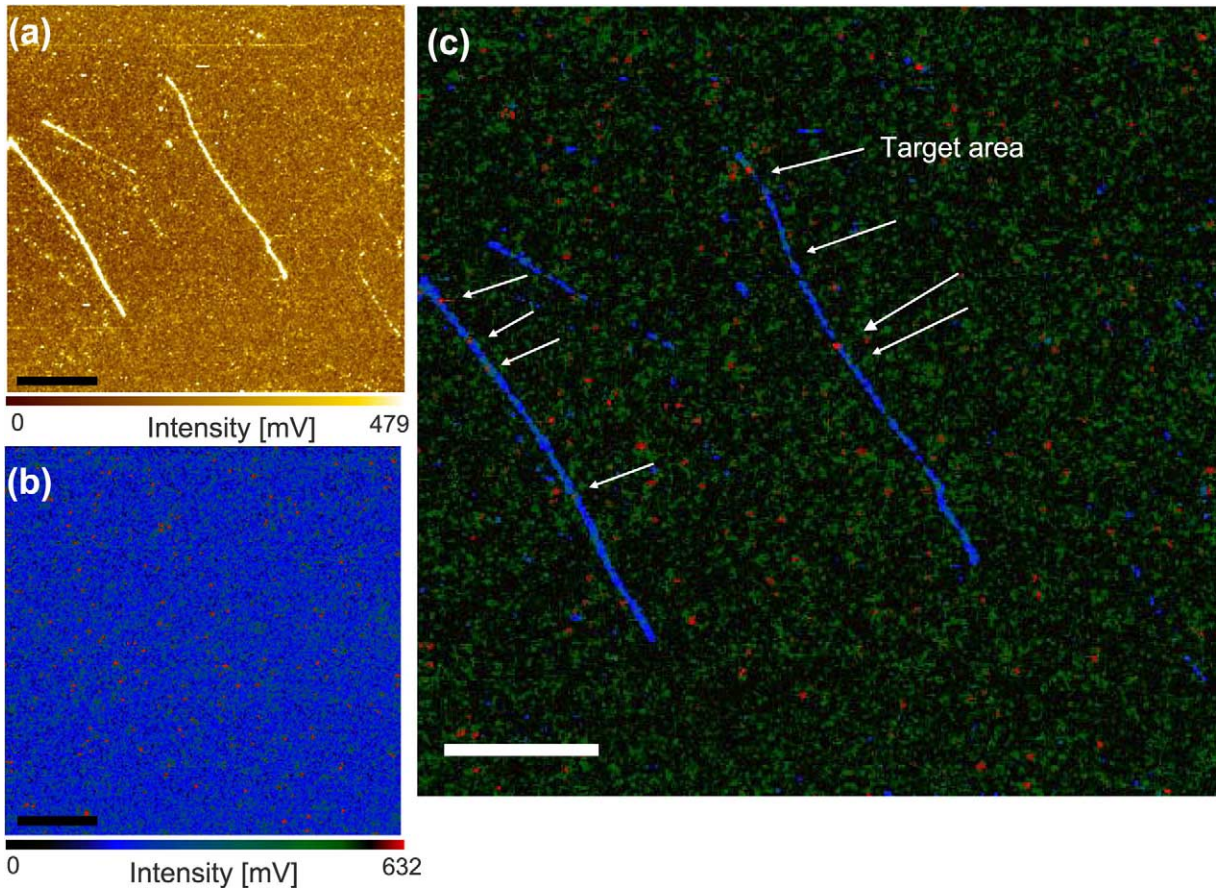

Fig. 3. Direct visualization of DNA abasic sites. YOYO-1 (a) and A532 (b) (λ_{exc} = 532 nm) fluorescence images were scanned separately to obtain abasic sites (c) where blue and red signals are from YOYO-1 and A532 dye molecules, respectively. In c, the target has a width of over 400 nm and shows strong fluorescence intensity at a FWHM. Scale bars correspond to 5 μm. A fluorescence signal of 1 V corresponds to 125 C/10 ms.

resolution (< 100 nm). This is not due to differences in the preparation of the sample since we have applied the same mixing ratio of dye and bp as in the previous report, but due to the high throughput efficiency of the optical fiber probe [17]. From the background signals (free YOYO-1 molecules) as shown in the dashed circle area in Fig. 2, it can be seen that the fluorescence widths of the free dye molecules and the widths of the DNA fluorescence signals are not same. This is an interesting phenomenon since the intercalation geometry of YOYO-1 is limited by the DNA width, and the DNA width is very small compared with the aperture size. Additionally, this is a common phenomenon with DNA fluorescence images derived from far-field microscopy. For example, the fluorescence DNA widths of YOYO-1 intercalated DNA molecules generally exceed the far-field optical resolution by more than two-fold (data not shown, or see [14]). In this image, the difference in the fluorescence widths between the modulated background signals (ca. 90 nm) and the DNA molecule (ca. 300 nm) is more than three-fold at full width half maximums (FWHM). In order to obtain information concerning this variation, it is necessary to obtain more high-resolution images.

Fig. 3 shows high-resolution near-field fluorescence images for the λ-DNA molecules containing abasic sites in 25×25 μm^2 image scales. The imaging was performed separately as a sequence of A532 dye (b) and YOYO-1 (a) to minimize the fluorescence energy transfer [21] of YOYO-1 to A532 molecules. The whole length of the DNA molecule was evaluated to about 17.5 μm in Fig. 3a. By superimposing the A532 image (b) on the YOYO-1 image (a), the abasic sites on DNA molecule were resolved as shown in Fig. 3c. The global appearance of the image, i.e. the length of the DNA molecules and the number of abasic light spots, is similar to the first report concerning the detection of abasic sites on λ-DNA molecules as determined by far-field fluorescence microscopy [11] since the experimental conditions used were similar. Five or six damaged sites were detected in the DNA molecules in both cases. Careful inspection for abasic sites is necessary since the size and intensity of the A532 light spots are not same. As compared with small and weak light signals from free A532 molecules and other abasic sites, the signals from the few abasic sites present are broad and strong. In an effort to obtain more information, we enlarged a strong light spot, denoted as 'Target' in Fig. 3c.

Fig. 4 shows the enlarged near-field fluorescence images representing scanned areas of 10×10 μm^2 (Fig. 4a,b,e), 2.5×2.5 μm^2 (Fig. 4c,d,f) and 1.5×1.5 μm^2 (Fig. 4g). Originally scanned images are shown in Fig. 4a,c for YOYO-1, and Fig. 4b,d for A532 dye, while Fig. 4e,f shows synthesized images for each scan area. Big light spots were still discernible in the originally scanned images for the YOYO-1 and A532 (Fig. 4a–d), consistent with Fig. 3. Additionally, a few small light spots become visible only when the images were enlarged. When the scan area was wide, for example 25×25

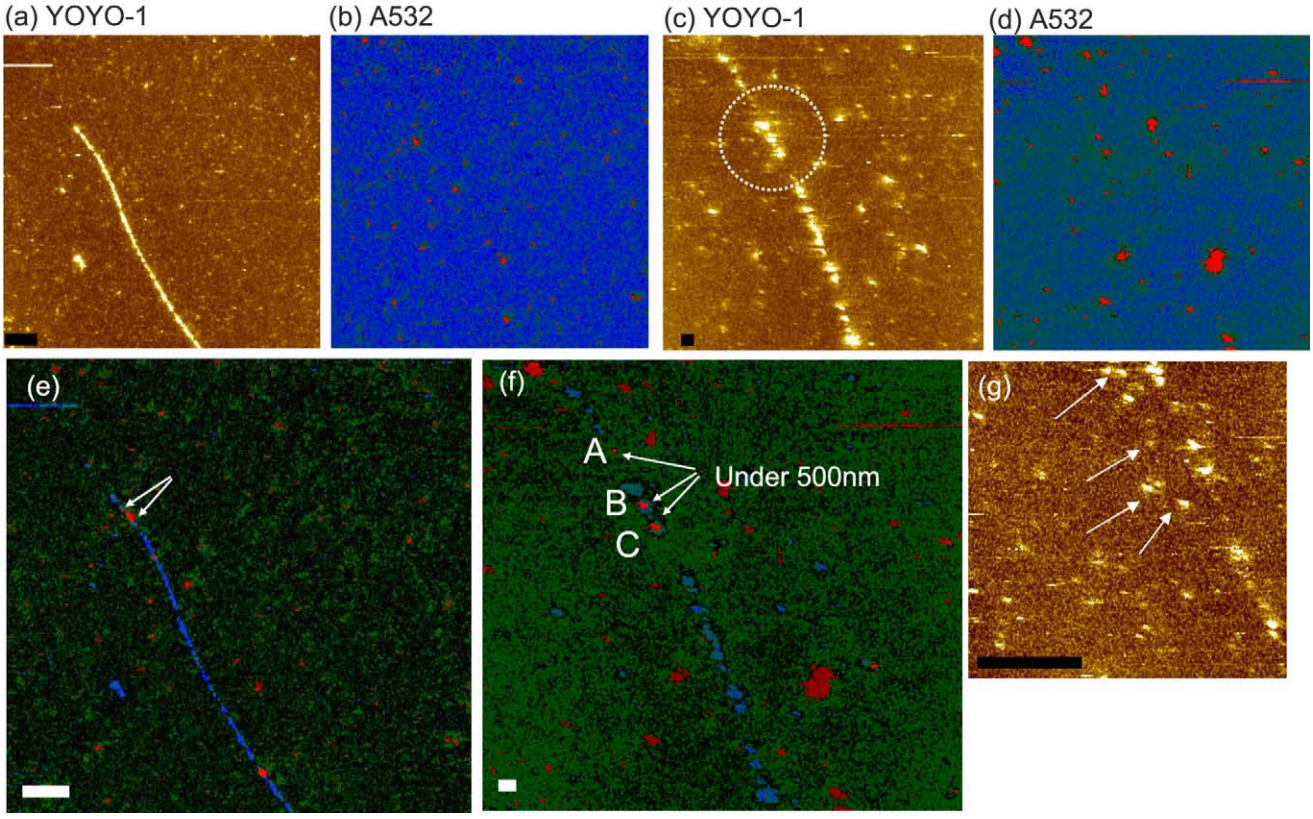

Fig. 4. Enlarged near-field fluorescence images for YOYO-1 (a,c,g) and A532 dye (b,d). e,f: Images derived for 10 μm^2 (a,b) and 2.5 μm^2 (c,d) scan areas, respectively. g: The enlarged area denoted by a dashed circle in c. Scale bars correspond to 1 μm (a,b,e) and 100 nm (c,d,f,g).

μm^2, 1 pixel of data point corresponded to approximately 50 nm of real distance in a horizontal direction since the data format was composed of 512 pixels and 256 lines. Consequently, if there is 1 pixel of signal missing, a 50 nm image distance cannot be detected in the 25 μm single line. Similarly, in the 2.5×2.5 μm^2 scan area, 1 pixel corresponded to approximately 5 nm of real distance. Therefore, a 1 pixel signal error does not significantly affect the resultant fluorescence images. This is a general problem in high-resolution scanning probe microscopy imaging as well as in high-resolution near-field imaging. In the case of near-field optical imaging, single molecular dynamics [22] can also influence the resultant near-field images. Fig. 4g shows an enlarged image (1.5×1.5 μm^2) of the YOYO-1 signals corresponding to the dashed circle area in Fig. 4c. At this scale, it is clearly shown that the original single line shaped fluorescence signals of YOYO-1 are completely separated. The bulk light spots in Fig. 4g, denoted by the arrows, are believed to be due to the presence of free YOYO-1 molecules on surface of the substrate. Similar results were obtained by simultaneous topographic and fluorescence imaging for YOYO-1 intercalated λ-DNA molecules (data not shown). This suggests that the deviation in fluorescence widths between the free YOYO-1 molecules and the DNA widths can be accounted for by the low pixel resolution when the scan area is wide. Using the same method for the preparation of images as shown in Fig. 4e,f, it can be seen that the target abasic spots were resolved separately within a 500 nm area. Three spots were resolved in Fig. 4f, and show different fluorescence characteristics. The shortest distance between two light spots is about 120 nm. We are unable to determine how many excited A532 molecules are involved in each light spot with the present data. On the other hand, in the photo-dissociation experiment for the single A532 molecule, more than eight consecutive scans were required using a similar optical probe with aperture size of approximately 25 nm (data not shown). Therefore, the signal separation of the A532 light spot cannot be accounted for by the photo-dissociation of a single dye molecule. Given that four A532 molecules can potentially be conjugated with streptavidin, this does not raise the specter of sudden photo-dissociation (see the instruction manual for s11224).

The optical resolution of the optical fiber probe used for single A532 molecules scattered at the surface was measured in an effort to obtain more detailed information (Fig. 5). The sample was prepared following standard procedures used for single molecule observation [1] in which PMMA was mixed with A532 molecules and spin-coated on a glass substrate. Since our purpose was only to confirm the fluorescence resolution, we did not confirm the number of excited molecules for the specific light spots. As can be seen in Fig. 5a, five light spots are present in the image. Line profile analyses yielded optical resolutions of 13 and 21 nm for the *X*-axis and *Y*-axis directions, respectively, as shown in Fig. 5b. The values are similar to those determined from Fig. 4c, d or g), however the error ranges are within 10%. The signal intensity of the light spots corresponds to about 430 mV (1 V = 125 C/10 ms), which is similar to the intensity of spot 'A' in Fig. 4f. Light spots 'B' and 'C' show a signal intensity of approximately 720 mV. If we assume an optical efficiency difference of 10% for single A532 molecules (see the manufacturer's document for A532 dye) for their entire lifetime, light spots 'B' and 'C' consisted of more than double the number of excited mole-

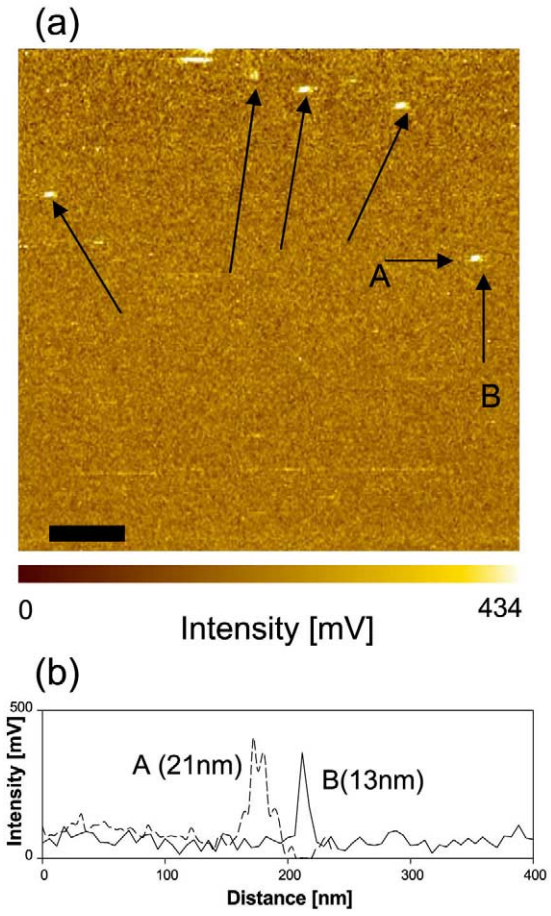

Fig. 5. a: Confirmation of near-field fluorescence resolution for A532 dye molecules. Scale bar corresponds to 100 nm. 'A' and 'B' indicate the line profile analysis directions shown in b.

cules compared to light spot 'A'. However, the number of excited molecules does not necessarily relate to the number of abasic sites since the number of conjugated A532 molecules can vary with each streptavidin. And therefore, at least more than three damage sites are located in the A532 light spots noted 'A' through 'C'. More thorough inspections are required in order to determine the exact number of abasic sites or excited dye molecules.

Recently, Sun et al. reported an AFM method for detecting abasic sites [23]. They detected two abasic sites on a 250 bp DNA template. In contrast, the SNOM method can be applied to relatively long DNA molecules, and requires only standard laboratory preparation techniques. Although we could not obtain a simultaneous topographic image by the rough surface, the topographic image can be replaced by using YOYO-1 fluorescence imaging.

In conclusion, we have investigated DNA abasic sites by the fluorescence labeling technique combined with the high-resolution near-field optical technique. To our knowledge, this is the first report dealing with the investigation of abasic DNA sites at sub-micron scale using optical techniques. We believe that high-resolution near-field imaging on middle- to short-length DNA samples can be helpful in the areas of DNA diagnosis and genetic studies.

Acknowledgements: The authors are grateful for the financial assistance provided by a Grant-In-Aid for the Center of Excellence (COE) Research, Japan.

References

[1] Dunn, R.C. (1999) Chem. Rev. 99, 2891–2927.
[2] Muramatsu, H., Chiba, N., Ataka, T., Monobe, H. and Fujihira, M. (1995) Ultramicroscopy 57, 141–146.
[3] Lhomme, J., Constant, J.F. and Demeunynck, M. (1999) Biopolymer 52, 65–83.
[4] Beger, R.D. and Bolton, P.H. (1998) J. Biol. Chem. 273, 15565–15573.
[5] Friedberg, E.C., Walkers, G.C. and Siede, W. (1995) DNA Repair and Mutagenesis. ASM Press, Washington DC.
[6] Kubo, K., Ide, H., Wallace, S.S. and Kow, Y.W. (1992) Biochemistry 31, 3703–3708.
[7] Meng, X., Benson, K., Chada, K., Huff, E.J. and Schwartz, D.C. (1995) Nat. Genet. 9, 432–438.
[8] Rossi, O., Carrozzino, F., Cappelli, E., Carli, F. and Frosina, G. (2000) Int. J. Cancer 85, 21–26.
[9] Michalet, X., Ekong, R., Fougerousse, F., Rousseaux, S., Schurra, C., Hornigold, N., van Slegtenhorst, M., Wolfe, J., Povey, S., Beckmann, J.S. and Bensimon, A. (1997) Science 277, 1518–1523.
[10] Lin, J., Qi, R., Aston, C., Jing, J., Anantharaman, T.S., Mishra, B., White, O., Daly, M.J., Minton, K.W., Venter, J.C. and Schwartz, D.C. (1999) Science 285, 1558–1562.
[11] Hirose, T., Ohtani, T., Muramatsu, H. and Tanaka, A. (2002) Photochem. Photobiol. 76, 123–126.
[12] Winkler, R., Perner, B., Rapp, A., Durm, M., Cremer, C., Greulich, K.-O. and Hausemann, M. (2003) J. Microsc. 209, 23–33.
[13] Yokota, H., Sunwoo, J., Sarikaya, M., Engh, G-v-d. and Aebersold, R. (1999) Anal. Chem. 71, 4418–4422.
[14] Lyubchenko, Y.L., Jacobs, B.L. and Lindsay, S.M. (1993) Proc. Natl. Sci. USA USA 90, 2137–2140.
[15] Kim, J.M., Ohtani, T., Sugiyama, S., Hirose, T. and Muramatsu, H. (2001) Anal. Chem. 73, 5984–5991.
[16] Muramatsu, H., Chiba, N. and Fujihira, M. (1997) Appl. Phys. Lett. 71, 2061–2063.
[17] Hosaka, N. and Saiki, T. (2001) J. Microsc. 202, 362–364.
[18] Bennink, M.L., Schärer, O.D., Lanaar, R., Sakata-Sogawa, K., Schins, J.M., Johannes, S.K., de Grooth, B.G. and Greve, J. (1999) Cytometry 36, 200–208.
[19] Nakao, H., Hayashi, H., Yoshino, T., Sugiyama, S., Otobe, K. and Ohtani, T. (2002) Nano Lett. 2, 475–479.
[20] Muramatsu, H., Homma, K., Yamamoto, N., Wang, J., Sakata-Sogawa, K. and Shimamoto, N. (2000) Mater. Sci. Eng. C 12, 29–32.
[21] Weiss, S. (1999) Science 283, 1676–1683.
[22] Dickson, R.M., Cubitt, A.B., Tsien, R.Y. and Moerner, W.E. (1997) Nature 388, 355–358.
[23] Sun, H.B. and Yokota, H. (2001) Anal. Chem. 73, 2229–2232.